

# Design of a $2 \times 1$ multiplexer with a ring resonator based on 2D photonic crystals

Fariborz Parandin\*, Nila Bagheri

*Department of Electrical Engineering, Kermanshah Branch, Islamic Azad University, Kermanshah, Iran*



## ARTICLE INFO

### Keywords:

Multiplexer  
Photonic crystal  
Ring resonator  
Photonic band gap

## ABSTRACT

Multiplexers are widely used logic circuits that connect a number of inputs to an output. These circuits are used to create logic functions. This article designs and simulates a  $2 \times 1$  multiplexer based on 2D photonic crystals. The structure of this multiplexer includes dielectric rods in an air background. At the input, there is a ring resonator between two waveguides. This multiplexer's structure is relatively small, with  $14 \times 15$  rods. The operating wavelength of this logic circuit is  $1.55 \mu\text{m}$ , which falls within the photonic band gap. The PWE method was used to simulate the band structure, and the FDTD numerical calculation method was used to calculate time.

## 1. Introduction

The increased speed of communication and information processing has resulted from the increased volume of information exchange and the growth of communication. All supporters of the electronic field strive for small size, fast speed, and low system error. This has sparked increased interest in optical electronics. Photonic crystals are among the most effective materials for designing and realizing optical integrated circuits. These heterogeneous materials, whose equivalent dielectric constant varies as a function of position, are the result of the repetition and alternation of a main cell and can have an effect on photon emission properties (Lalbakhsh et al., 2021; Roshani and Roshani, 2020; Jamshidi et al., 2021; Jamshidi et al., 2019; Lalbakhsh et al., 2021; Roshani et al., 2020; Lalbakhsh et al., 2022; Hadei et al., 2022; Adibi et al., 2021; Karambasti et al., 2022).

Photonic crystals are periodic dielectric structures that do not allow light of a specific wavelength to pass through them, allowing light to pass through the structure by forming a waveguide. This feature can be used to build many gates and logic circuits with proper design. The wavelength range that does not pass through the structure is referred to as the photonic band gap. The forbidden photonic band's wavelength range is determined by crystal structure properties such as rod type and radius, as well as the lattice constant. The distance between the centers of two adjacent rods is defined as the lattice constant. Fine bends are not an issue in the design of photonic crystals because their performance is based on the photonic band gap rather than total reflection laws. Because of their small dimensions and ability to design multiple logic

circuits, photonic crystals are well suited for integration. Photonic crystal structures can be one-dimensional, two-dimensional, or three-dimensional, with a one-, two-, or three-dimensional refractive index sequence (Farmani et al., 2019; Farmani, 2017; Olyae and Taghipour, 2011; Olyae et al., 2018; Vahdati and Parandin, 2019; Mohebzadeh-Bahabady and Olyae, 2018; Askarian et al., 2019; Askarian and Akbarizadeh, 2022; Parandin and Moayed, 2020; Rezaei et al., 2020).

Photonic crystals have been used to create numerous analog and digital circuits because they are particularly adaptable for optical designs. Analog circuitry includes optical sensors and filters. Logic gates and various types of combinational and sequential circuits are examples of digital circuits. Photonic crystals were previously used to make circuits such as multiplexers, encoders, decoders, and various types of flip-flops. Circuit dimensions are an important consideration in these designs. When an optical circuit's size is reduced, it can be used in optical integrated circuits. The difference between two logical values of 0 and 1 is another important parameter. In both cases, increasing the power difference lowers the bit detection error (Parandin and Sheykhanian, 2022; Askarian et al., 2019; Serajmohammadi et al., 2015; Askarian et al., 2020; Parandin et al., 2021; Seraj et al., 2020; Parandin, 2021; Naghizade and Saghaei, 2002; Parandin and Malmir, 2020; Karkhanehchi et al., 2017; Sani et al., 2020; Parandin et al., 2021; Sonth et al., 2018; Serajmohammadi et al., 2018; Parandin et al., 2022; Seifouri et al., 2019; Parandin and Sheykhanian, 2022; Jalali-Azizpoor et al., 2018; Parandin et al., 2022). Ring resonators have been used in some of these structures. The larger the number of these rings, the longer the delay time and the size of the design (Radhouene et al., 2022; Thirumaran

\* Corresponding author.

E-mail address: [fa.parandin@iau.ac.ir](mailto:fa.parandin@iau.ac.ir) (F. Parandin).

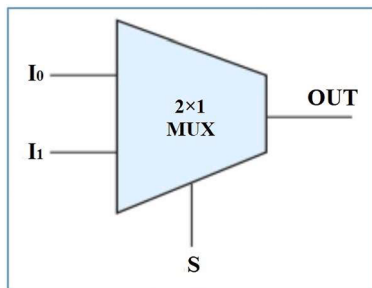


Fig. 1. Multiplexer's block diagram.

Table 1

The truth table for multiplexer.

S	A	B	Output
0	0	0	0
0	1	0	1
0	0	1	0
0	1	1	1
1	0	0	0
1	1	0	0
1	0	1	1
1	1	1	1

et al., 2021; Zhang et al., 2014; Parandin and Sheykhan, 2022; Masilamani and Punniakodi, 2020).

Access to high-speed communication structures and devices, as well as high-capacity and bandwidth channels, are among the most critical requirements of today's telecommunications systems. Unlike structures based on total reflection, these structures do not have issues with minor bends. The circuit dimensions are extremely small, and integration is possible. One technique for maximizing the benefit of a communications channel's capacity is wavelength division. As a result, many wavelengths are multiplexed for transmission in a telecommunication channel, and at the destination, different wavelengths are separated by a demultiplexer. As a result, multiplexers are widely used logic circuits in telecommunications and processors. In addition to inputs, these circuits use selection lines. The selection line indicates which input should be routed to which output.

Until now, photonic crystal structures for optical multiplexers have been limited. The dimensions of the majority of these structures are large, making them unsuitable for optical integrated circuits. Furthermore, some of them have a long delay time, which slows down information transfer (Wang et al., 2019; Nawwar et al., 2018; Selim et al., 2010; Fasihi and Bashiri, 2020; Zhao et al., 2019; Rao et al., 2021).

The goal of this paper is to design a fast, small, and high-precision multiplexer. There is an acceptable difference between the lowest logic 1 value and the highest logic 0 value. This lowers error and demonstrates the circuit's high precision.

This structure is simulated using RSOFT software. To simulate the proposed structure, Full-Wave and Band-Solve modules were used. The Band-Solve module and the Plane Wave Expansion (PWE) method were used to generate the band structure results. The Full-Wave module and the Finite Difference Time Domain method were used to calculate time.

## 2. Multiplexer function

The two broad categories of logical circuits are combinational circuits and sequential circuits. Multiplexers are combinational logic circuits that switch from multiple input lines to a single output. Multiplexing is the process of transmitting one or more signals over a single transmission line. Multiplexing is achieved by employing a selection line or lines. Each multiplexer has  $n^2$  inputs,  $n$  selection lines, and one output. The values that are passed from the input to the output are

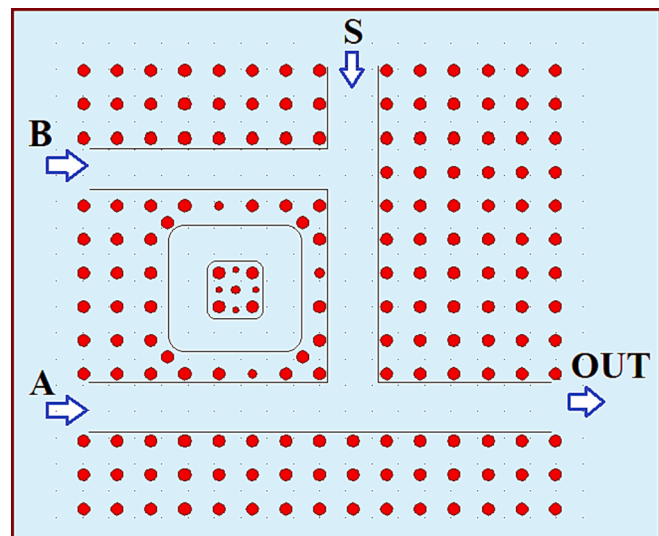


Fig. 2. Proposed structure for  $2 \times 1$  optical multiplexer.

determined by the selection lines (Fig. 1).

Table 1 shows the truth table for this multiplexer. The table shows that three input variables are considered, resulting in eight possible states, defined as follows.

The output function of a  $2 \times 1$  multiplexer can be expressed in terms of inputs and selection line as shown in the table as:  $M = A.S' + B.S$ .

If the selection line becomes zero, the first line (A) is transferred to the output and if it becomes 1, the second output (B) is transferred to the output, and the output of the circuit would be proportional to that input.

## 3. Optical multiplexer design

Because optical circuits must function properly, much attention has been paid to their design and the modification of their main properties, such as increasing speed, decreasing size, increasing accuracy, and increasing integration potential. This article simulates a 2 to 1 optical multiplexer based on 2D photonic crystals and a ring resonator. Fig. 2 depicts a multiplexer made up of three waveguides and a ring resonator. This is a square structure with  $14 \times 15$  silicon rods with a refractive index of 3.4 in an air background (refractive index of 1). The radius of the rods is 115 nm, and the lattice constant is 0.64  $\mu\text{m}$ .

The ring resonator acts as a coupling element between the waveguides. A ring resonator has a specific resonant wavelength. The waves emitted at this wavelength are coupled in the ring and can propagate to other waveguides. The ring resonator can direct the amount of coupled power to the output path, which increases the output power, which is useful when the output must be in logic 1. Also, in some structures, depending on the condition of the inputs, the ring can direct the optical power to other input paths and reduce the output power, which is useful when the output must be in logic 0. The interaction of light and rods determines light emission in the ring. Changing the rod radius in the ring resonator can thus affect the power in waveguides. Thus, different simulations were used to determine the best radius of the rods to reduce power in mode 0 and increase power in mode 1. The radius of three rods in the wall between the ring resonator and the waveguides is reduced so that the radius of two of them is 0.7 and the radius of one is 0.8 of the initial radius. Four rods with radius of  $0.5r$  have been placed in the center of the ring, each with a radius coefficient of  $0.7r$ . The simulations show that decreasing the radius of these rods improves the results. A phase difference of  $-70^\circ$  was applied to input source A and a phase difference of  $10^\circ$  was applied to output source B to improve the outputs.

One of the photonic crystal's properties is that it prevents certain light wavelengths from passing through. As a result, it is possible to

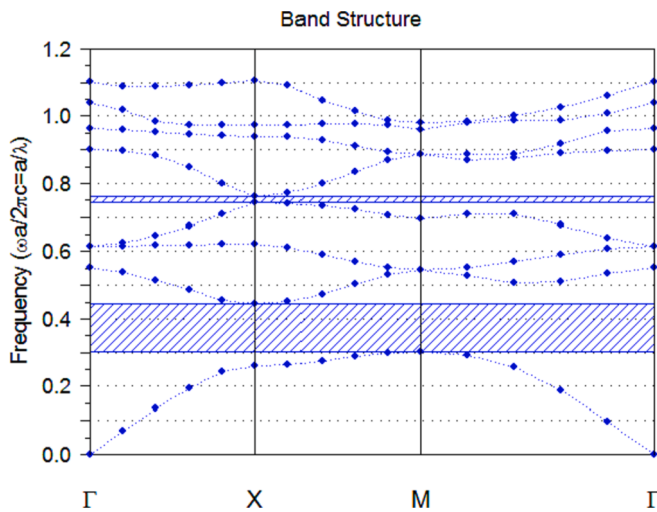


Fig. 3. Photonic band gap diagram for the photonic crystal structure.

prevent the emission of a wide range of wavelengths by designing a photonic crystal structure. These wavelengths are referred to as photonic band gaps. The physical properties of the photonic crystal structure can be changed to change the wavelengths. Some of these wavelengths can be guided and controlled in that direction by forming a

waveguide in a photonic crystal.

The wavelength range of the structure's photonic band gap is effectively determined by the values of the rods' radius and lattice constant, as well as their type and refractive index. As a result of determining the characteristics, the wavelength range of the photonic band gap is determined to be in the range of  $39 \mu\text{m} < \lambda < 1.88 \mu\text{m}$ . As can be seen, the multiplexer's operating wavelength in this range is  $1.55 \mu\text{m}$ . Fig. 3 depicts the band gap diagram of this circuit's structure.

A selection line and two inputs are provided by the  $2 \times 1$  multiplexer. The selection line determines which inputs are routed to the output. States  $S = 0$  and  $S = 1$  can be used to evaluate the performance of this circuit. In the case of  $S = 0$ , the input A is transferred to the output regardless of the value of the other input because it is 0 or 1. (B). Following that, we will examine all of the different states of the inputs and their resulting outputs.

In the first case,  $S = 0$  is considered. If  $A = B = 0$ , all of the input sources and the selection line are turned off, and no power is generated, so the power in the output is zero, and the output is logically set to 0.

If  $S = 0$ , the first input should be sent to the output. According to the simulation results, the normalized output power is approximately 0.60 in the case of  $A = 1$  and  $B = 0$ , which is equivalent to a logic value of 1. The optical power distribution in waveguides is depicted in Fig. 4(a), while the normalized output power is depicted in Fig. 4(b).

When optical power is applied to the inputs and reaches the output, the effect of all the inputs takes time to reach the output. As a result, a

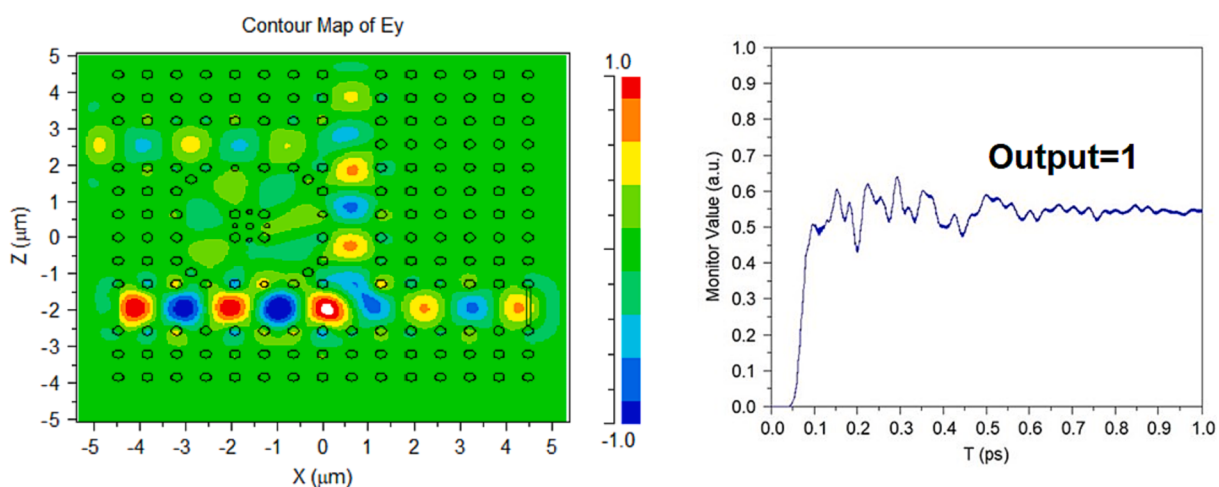


Fig. 4. a) Optical power distribution; b) output power diagram for  $s = 0$ ,  $A = 1$  and  $B = 0$ .

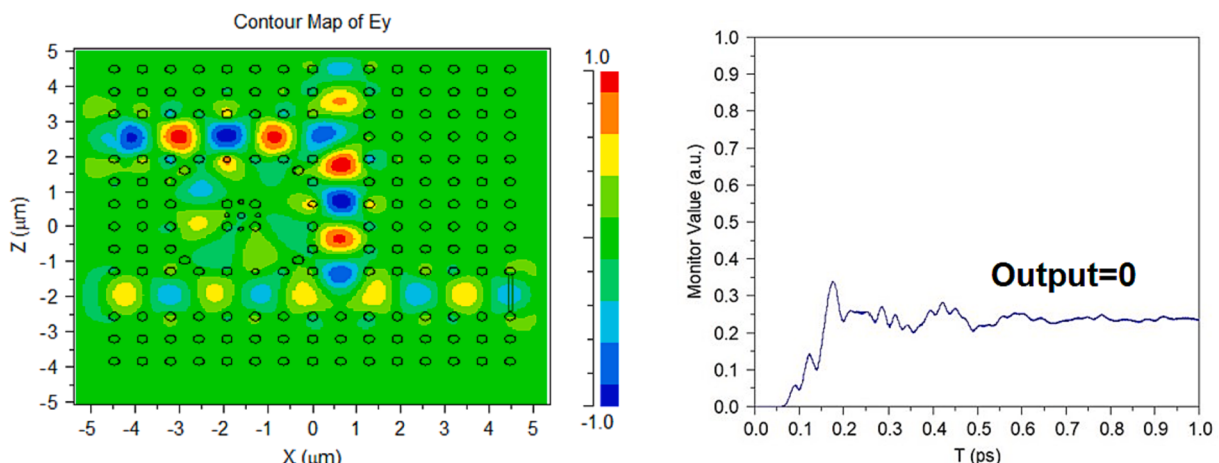
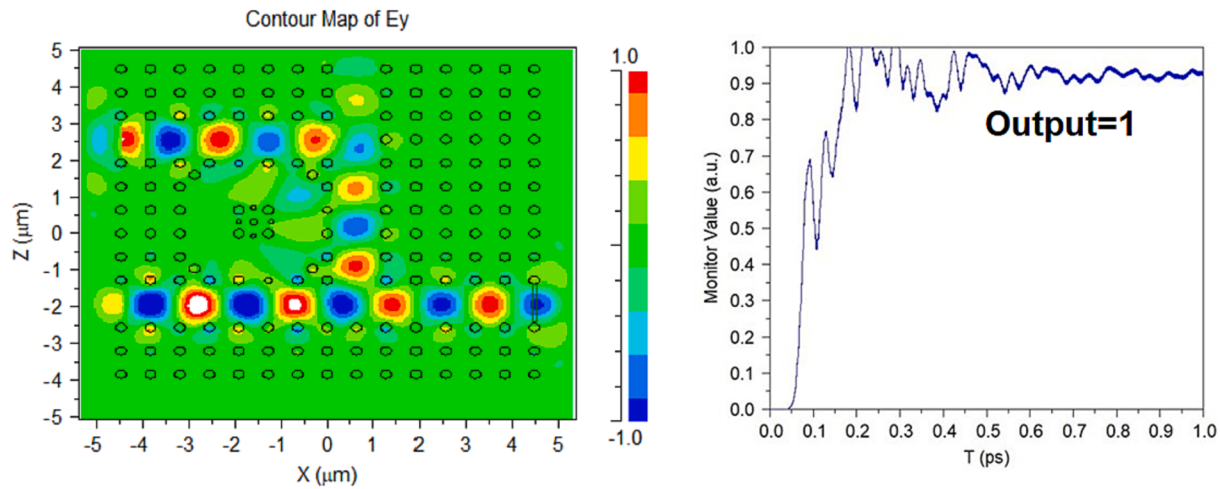
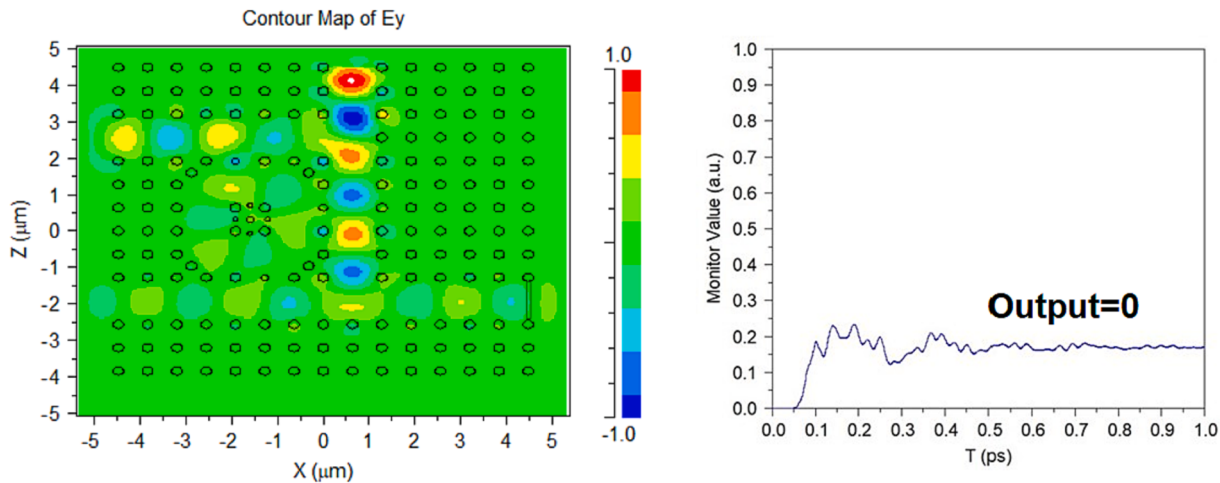


Fig. 5. a) Optical power distribution; b) output power diagram for  $s = 0$ ,  $A = 0$  and  $B = 1$ .



**Fig. 6.** A) Optical power distribution; b) output power diagram for  $s = 0$ ,  $A = B = 1$ .



**Fig. 7.** A) Optical power distribution; b) output power diagram for  $s = 1$ ,  $A = B = 0$ .

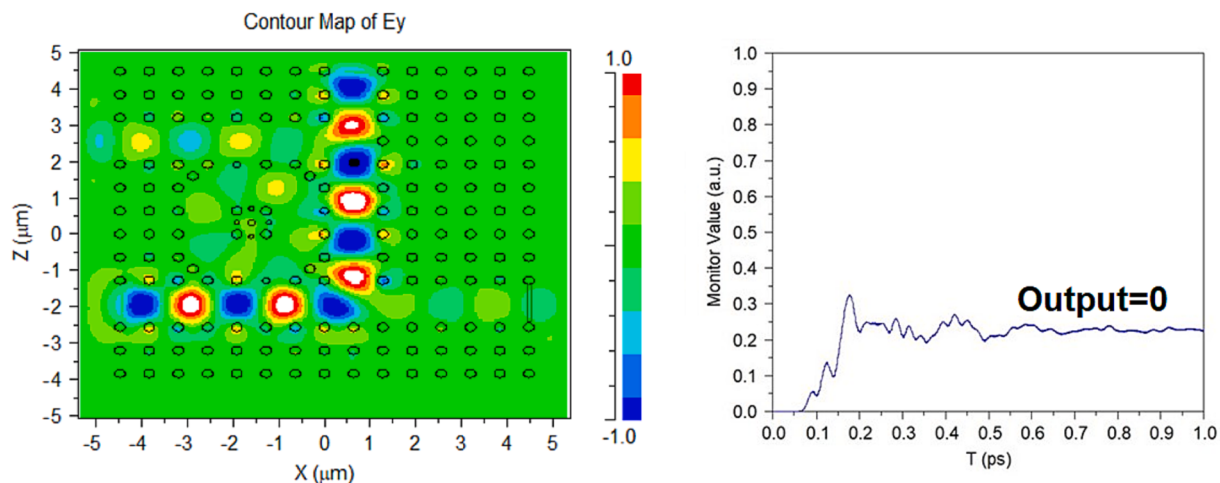


**Fig. 8.** A) Optical power distribution; b) output power diagram for  $s = 1$ ,  $A = 1$  and  $B = 0$ .

transition time is required for the output to reach a stable state. This time, like any other electronic circuit, must pass until the output reaches an almost constant value. This time can be reduced by using structures with few rings and small sizes.

The selection line remains unchanged, but the other two inputs have been changed to  $A = 0$  and  $B = 1$ . Fig. 5 shows the simulation as well as the final output graph. As expected, the output power is quite low, and the calculated normalized power in this case is around 0.25, which is

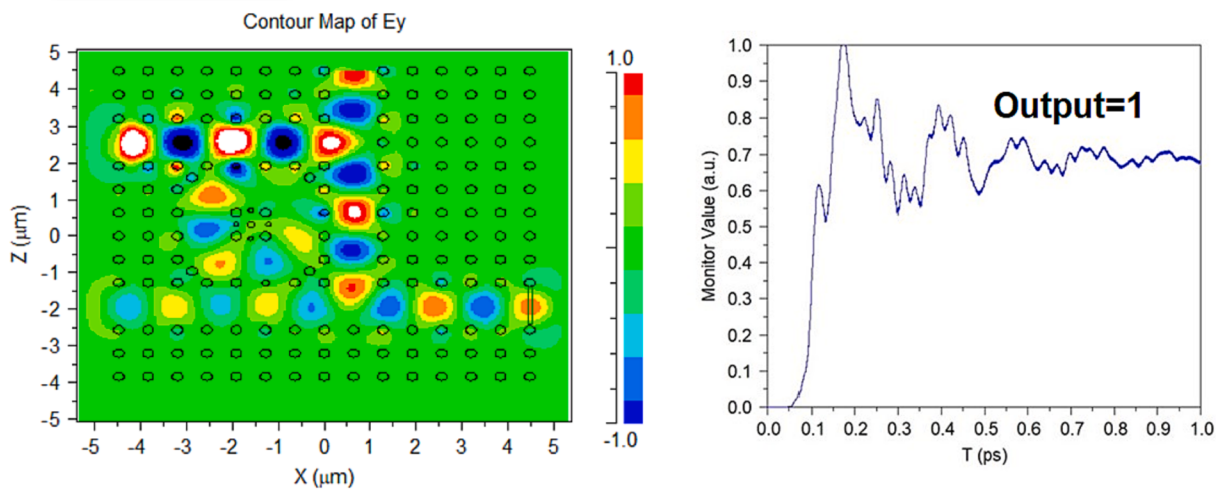


**Fig. 9.** A) Optical power distribution; b) output power diagram for  $s = 1$ ,  $A = 0$  and  $B = 1$ .

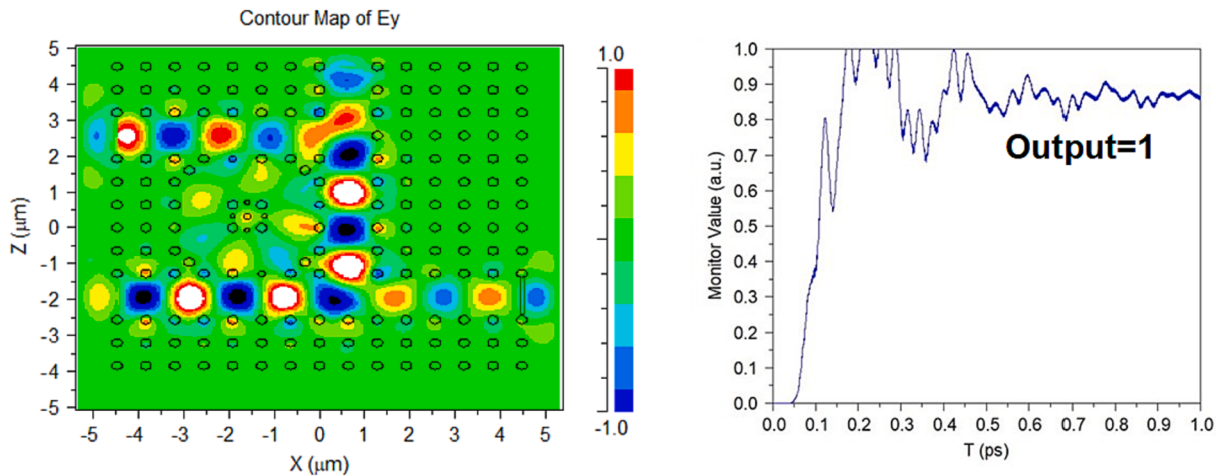


**Fig. 10.** A) Optical power distribution; b) output power diagram for  $s = 1$ ,  $A = B = 1$ .

comparable to logic 0. Fig. 5(a) shows the optical power distribution in this case, while Fig. 5(b) shows the normalized power distribution.

In the final case,  $S = 0$ , the inputs are assumed to be one, i.e.,  $A = B = 1$ . In this case, the output power is approximately 0.98, corresponding to a logic value of 1. The results of this simulation are depicted in Fig. 6.

In the following example, we assume the selection line's input is  $S = 1$ . In this scenario, the inputs have four states that we will investigate. Consider the case where  $A = 0$  and  $B = 0$  are the inputs. In this case, the normalized output power value is calculated to be 0.17, corresponding to a logic value of 0. Figs. 7 and 8 show the power distribution diagram

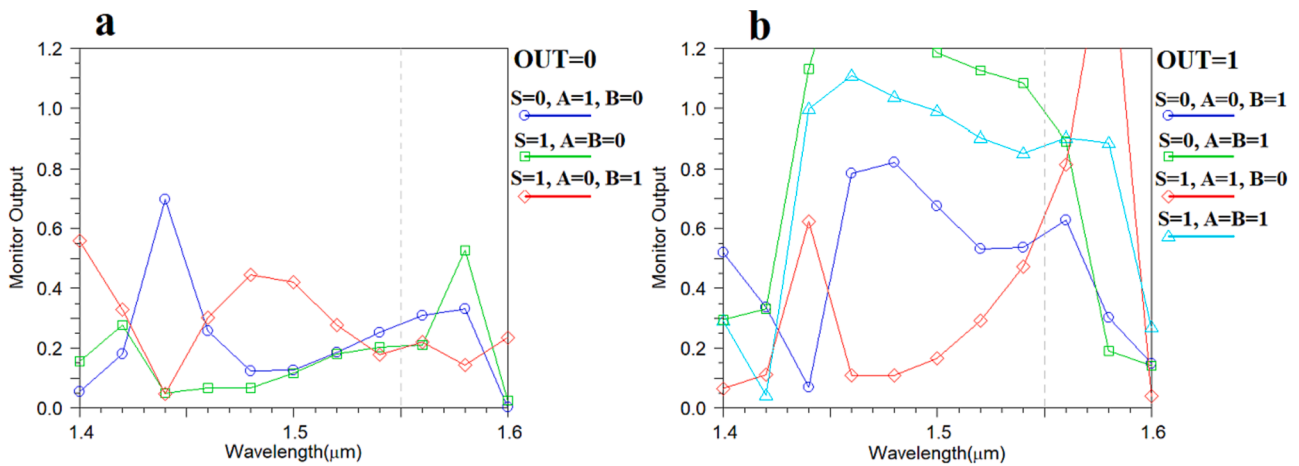


**Fig. 11.** A) Optical power distribution; b) output power diagram for  $s = 1$ ,  $A = B = 1$ .

**Table 2**

Comparison table of results with previous works.

Article	Number of rodes	Lattice constant (nm)	Stability Time (ps)	Min Power for 0 logic	Max Power for 1 logic	Wavelength (nm)	Number of sources
(Parandin and Sheykhan, 2022)	20 × 20	640	0.35	0.2	0.52	1550	3
(Fasihi and Bashiri, 2020)	47 × 27	580	>5	—	0.7	1581	3
(Zhao et al., 2019)	26 × 25	595	1	—	0.93	1551	3
(Rao et al., 2021)	15 × 13	600	0.2	0.2	0.55	1550	4
This Work	14 × 15	640	0.55	0.25	0.6	1550	3

and output normalized power for this state (a and b).

In the following example, we assume the selection line's input is  $S = 1$ . When  $S = 1$  and the inputs are  $A = 1$  and  $B = 0$ , the output is approximately 0.20, which is equivalent to a logic value of 0. The power distribution diagram and normalized power in the output for this state are shown in Fig. 8(a and b).

The values of the other two inputs are changed to  $A = 0$  and  $B = 1$ , while the input  $S$  remains unchanged. The output is anticipated to be 1, as the value of the input  $B$  changes to 1. Fig. 9 demonstrates that the numerical value of  $M = 1$ 's output value is 0.70.

The final state we evaluate for the selection line  $S = 1$  is  $A = B = 1$ . The output in this condition has a normalized power of approximately 0.87, corresponding to a logic value of 1. The power and output power distribution diagram for this state is shown in Fig. 10(a and b).

The simulation is performed, and the output is obtained for each mode to obtain the appropriate simulation wavelength in all possible input modes. Fig. 11(a) shows the results in state 0, and Fig. 11(b) shows the results in state 1. According to this figure, it can be seen that the outputs in mode 0 have the lowest power and the outputs have the highest power in mode 1 for the wavelength of 1.55 μm.

The results show that the optical power of the worst value of 1 is equal to 0.6 and that of the worst value of 0 is equal to 0.25. Therefore, 0.3 and 0.55, respectively, can be thought of as the acceptable levels for values of 0 and 1. The proposed structure in this study was compared with some of other proposed multiplexers in order to obtain its advantages, and the results are shown in Table 2.

The multiplexer in reference (Parandin and Sheykhan, 2022) has a short delay time, but Table 2 reveals that it has larger dimensions than the suggested structure. Additionally, in the suggested design, mode 1's power value increased. It can be said that the proposed structure is much smaller and that the time to reach the stable state is much shorter than references (Fasihi and Bashiri, 2020; Zhao et al., 2019). The proposed structure is the same size as Reference (Rao et al., 2021), but Reference (Rao et al., 2021) has a shorter delay time. However, this structure uses a second source, which increases power usage. Additionally, compared to the referenced design, the one proposed in this article has more power in logical mode 1.

#### 4. Conclusion

In this paper, a ring resonator-based 2D photonic crystal  $2 \times 1$  multiplexer is built and simulated. For this, a small, straightforward square structure with high speed and accuracy is used. The structure consists of a ring resonator and three waveguides. A small size photonic crystal structure is used in the proposed design. This structure is designed for the wavelength of 1550 nm, which is used in optical fiber communication. The simulation results show that the proposed structure has a stability time of 0.55 ps. According to this simulation results, this structure is suitable for high precision optical integrated circuits and has an acceptable difference between two logical values of 0 and 1.

#### Declaration of Competing Interest

The authors declare that they have no known competing financial interests or personal relationships that could have appeared to influence

the work reported in this paper.

#### Data availability

No data was used for the research described in the article.

#### References

- Adibi, S., Amin Honarvar, M., Lalbakhsh, A., 2021. Gain enhancement of wideband circularly polarized UWB Antenna using FSS. *Radio Sci.* 56 e2020RS007098.
- Askarian, A., Akbarizadeh, G., Fartash, M., 2019. All-optical half-subtractor based on photonic crystals. *Appl. Opt.* 58, 5931–5935.
- Askarian, A., Akbarizadeh, G., Fartash, M., 2019. A novel proposal for all optical half-subtractor based on photonic crystals. *Opt. Quantum Electron.* 51 (8), 264–272.
- Askarian, A., Akbarizadeh, G., Fartash, M., 2020. An all-optical half subtractor based on Kerr effect and photonic crystals. *Optik* 207, 164424.
- Askarian, A., Akbarizadeh, G., 2022. A novel proposal for all optical  $2 \times 4$  decoder based on photonic crystal and threshold switching method. *Opt. Quant. Electron.* 54, 84.
- Farmani, A., 2017. Quantum-dot semiconductor optical amplifier: performance and application for optical logic gates. *Majlesi J. Telecommun. Devices* 6 (3), 93–97.
- Farmani, A., Mir, A., Irannejad, M., 2019. 2D-FDTD simulation of ultra-compact multifunctional logic gates with nonlinear photonic crystal. *J. Opt. Soc. Am. B* 36 (4), 811–818.
- Fasihi, K., Bashiri, S., 2020. A new  $2 \times 1$  photonic crystal multiplexer assisted by Fano resonances and Kerr nonlinear effect. *Photon. Nanostruct.-Fund. Appl.* 42, 100837.
- Hadei, M., Dadashzadeh, G., Torabi, Y., Lalbakhsh, A., 2022. Terahertz beamforming network with a nonuniform contour. *Appl. Opt.* 61 (4), 1087–1096.
- Jalali-Azizpoor, M.R., Soroosh, M., Seifi-Kavian, Y., 2018. Application of self-collimated beams in realizing all-optical photonic crystal-based half-adder. *Photon Netw. Commun.* 36, 344–349.
- Jamshidi, M.B., Siahkamari, H., Roshani, S., Roshani, S., 2019. A compact Gysel power divider design using U-shaped and T-shaped resonators with harmonics suppression. *Electromagnetics* 39 (7), 491–504.
- Jamshidi, M.B., Roshani, S., Talla, J., Roshani, S., Peroutka, Z., 2021. Size reduction and performance improvement of a microstrip Wilkinson power divider using a hybrid design technique. *Sci. Rep.* 11, 7773.
- Karambasi, B.M., Ghodrat, M., Ghorbani, G., Lalbakhsh, A., Behnia, M., 2022. Design methodology and multi-objective optimization of small-scale power-water production based on integration of Stirling engine and multi-effect evaporation desalination system. *Desalination* 526, 115542.
- Karkhanechi, M.M., Parandin, F., Zahedi, A., 2017. Design of an all optical half-adder based on 2D photonic crystals. *Photon Netw. Commun.* 33, 159–165.
- Lalbakhsh, A., Afzal, M.U., Hayat, T., Esselle, K.P., Manda, K., 2021. All-metal wideband metasurface for near-field transformation of medium-to-high gain electromagnetic sources. *Sci. Rep.* 11 (1), 1–9.
- Lalbakhsh, A., Mohamadpour, G., Roshani, S., Ami, M., Roshani, S., Sayem, A.S.M.D., Alibakhshikenari, M., Koziel, S., 2021. Design of a compact planar transmission line for miniaturized rat-race coupler with harmonics suppression. *IEEE Access* 9, 129207–129217.
- Lalbakhsh, A., Simorangkir, R.B.V.B., Bayat-Makou, N., Kishk, A.A., Esselle, K.P., 2022. Advancements and artificial intelligence approaches in antennas for environmental sensing. *Artif. Intell. Data Sci. Environ. Sens.* 19–38.
- Masilamani, S., Punnakiodki, S., 2020. Photonic crystal ring resonator based optical MUX/DEMUX design structures: a survey and comparison study. *J. Opt.* 49, 168–177.
- Mohebzadeh-Bahabady, A., Olyaei, S., 2018. All-optical NOT and XOR logic gates using photonic crystal nano-resonator and based on an interference effect. *IET Optoelectron.* 12 (4), 191–195.
- Naghizade, S., Saghaei, H., 2020. A novel design of all-optical half adder using a linear defect in a square lattice rod-based photonic crystal microstructure, arXiv preprint arXiv, 2002.04535.
- Nawwar, O.M., Shalaby, H.M., Pokharel, R.K., 2018. Photonic crystal-based compact hybrid WDM/MDM (De) multiplexer for SOI platforms. *Opt. Lett.* 43 (17), 4176–4179.
- Olyaei, S., Taghipour, F., 2011. Design of new square-lattice photonic crystal fibers for optical communication applications. *Int. J. Phys. Sci.* 6 (18), 4405–4411.
- Olyaei, S., Seifouri, M., Mohebzadeh-Bahabady, A., Sardari, M., 2018. Realization of all-optical NOT and XOR logic gates based on interference effect with high contrast ratio and ultra-compacted size. *Opt. Quant. Electron.* 50, 385.

- Parandin, F., 2021. Ultra-compact terahertz all-optical logic comparator on GaAs photonic crystal platform. *Opt. Laser Technol.* 144, 107399.
- Parandin, F., Malmir, M.R., 2020. Reconfigurable all optical half adder and optical XOR and AND logic gates based on 2D photonic crystals. *Opt. Quant. Electron.* 52, 56.
- Parandin, F., Sheykhan, A., 2022. Design of an all-optical half adder based on photonic crystal ring resonator. *Opt. Quant. Electron.* 54, 443.
- Parandin, F., Kamarian, R., Jomour, M., 2021. Optical 1-bit comparator based on two-dimensional photonic crystals. *Appl. Opt.* 60, 2275–2280.
- Parandin, F., Heidari, F., Aslinezhad, M., et al., 2022. Design of 2D photonic crystal biosensor to detect blood components. *Opt. Quant. Electron.* 54, 618.
- Parandin, F., Moayed, M., 2020. Designing and simulation of 3-input majority gate based on two-dimensional photonic crystals. *Optik* 216, 164930.
- Parandin, F., Olyaei, S., Kamarian, R., Jomour, M., 2022. Design and simulation of linear all-optical comparator based on square-lattice photonic crystals. *Photonics* 9, 459.
- Parandin, F., Sheykhan, A., 2022. Designing a circuit for high-speed optical logic half subtractor. *Int. J. Circuits Syst. Signal Process.* 16, 887–891.
- Parandin, F., Sheykhan, A., 2022. Design and simulation of a  $2 \times 1$  All-Optical multiplexer based on photonic crystals. *Opt. Laser Technol.* 151, 108021.
- Parandin, F., Heidari, F., Rahimi, Z., Olyaei, S., 2021. Two-Dimensional photonic crystal biosensors: a review. *Opt. Laser Technol.* 144, 107397.
- Radhouene, M., Gharsallah, Z., Balaji, V.R., Najjar, M., Robinson, S., Janyani, V., Murugan, M., Hegde, G., Sridarshini, T., 2022. Design and analysis of a channel drop filter and demultiplexer based on a photonic crystal super ellipse-shaped ring resonator. *Laser Phys.* 32 (11), 116202.
- Rao, D.G.S., Swarnakar, S., Kumar, S., 2021. Design of photonic crystal based compact all-optical  $2 \times 1$  multiplexer for optical processing devices. *Microelectron. J.* 112, 105046.
- Rezaei, M.H., Boroumandi, R., Zarifkar, A., Farmani, A., 2020. Nano-scale multifunctional logic gate based on graphene/hexagonal boron nitride plasmonic waveguides. *IET Optoelectron.* 14 (1), 37–43.
- Roshani, S., Jamshidi, M.B., Mohebi, F., Roshani, S., 2020. Design and modeling of a compact power divider with squared resonators using artificial intelligence. *Wireless Personal Commun.* 117 (3), 2085–2096.
- Roshani, S., Roshani, S., 2020. Design of a high efficiency class-F power amplifier with large signal and small signal measurements. *Measurement* 149, 106991.
- Sani, M.H., Tabrizi, A.A., Saghaei, H., et al., 2020. An ultrafast all-optical half adder using nonlinear ring resonators in photonic crystal microstructure. *Opt. Quant. Electron.* 52, 107.
- Seifouri, M., Olyaei, S., Sardari, M., Mohebzadeh-Bahabady, A., 2019. Ultra-fast and compact all-optical half adder using 2D photonic crystals. *IET Optoelectron.* 13 (3), 139–143.
- Selim, R., Pinto, D., Obayya, S.S.A., 2010. Improved design of photonic crystal-based multiplexer/demultiplexer devices. *IET Optoelectron.* 4 (4), 165–173.
- Seraj, Z., Soroosh, M., Alaei-Sheini, N., 2020. Ultra-compact ultra-fast 1-bit comparator based on a two-dimensional nonlinear photonic crystal structure. *Appl. Opt.* 59, 811–816.
- Serajmohammadi, S., Alipour-Banaei, H., Mehdizadeh, F., 2015. All optical decoder switch based on photonic crystal ring resonators. *Opt. Quant. Electron.* 47, 1109–1115.
- Serajmohammadi, S., Alipour-Banaei, H., Mehdizadeh, F., 2018. Proposal for realizing an all-optical half adder based on photonic crystals. *Appl. Opt.* 57, 1617–1621.
- Sonth, M.V., Soma, S., Gowre, S.C., et al., 2018. Modeling and optimization of optical half adder in two dimensional photonic crystals. *J. Elec. Mater.* 47, 4136–4139.
- Thirumaran, S., Dhanabalan, S.S., Sannasi, I.G., 2021. Design and analysis of photonic crystal ring resonator based  $6 \times 6$  wavelength router for photonic integrated circuits. *IET Optoelectron.* 15 (1), 40–47.
- Vahdati, A., Parandin, F., 2019. Antenna patch design using a photonic crystal substrate at a frequency of 1.6 THz. *Wireless Personal Commun.* 109, 2213–2219.
- Wang, Y., Lv, H., Jiang, T., Zhang, K., 2019. Reconfigurable optical add-drop multiplexer at 1550 nm using magnetically-coupled switches based on a photonic crystal. *Optik* 192, 162878.
- Zhang, Y., Zeng, C., Li, D., Gao, G., Huang, Z., Yu, J., Xia, J., 2014. High-quality-factor photonic crystal ring resonator. *Opt. Lett.* 39, 1282–1285.
- Zhao, T., Asghari, M., Mehdizadeh, F., 2019. An all-optical digital 2-to-1 multiplexer using photonic crystal-based nonlinear ring resonators. *J. Electron. Mater.* 48, 2482–2486.